Ion transport through a T-intersection of nanofluidic channels

Hirofumi Daiguji, Takuma Adachi, and Naoya Tatsumi
Institute of Environmental Studies, The University of Tokyo, 5-1-5 Kashiwanoha, Kashiwa 277-8563
(Received 8 April 2008; published 1 August 2008)

Ion transport through a T-intersection of two silica nanochannels (a main channel, 5-μm long and 30-nm wide, and a subchannel, 5-μm long and 15-nm wide) with a surface charge distribution was investigated based on continuum dynamics calculations. The surface charge within 250 nm of the intersection in the main channel and the entire subchannel was positive and that in the main channel outside this intersection region was negative. This nanofluidic system is analogous to a *p-n-p* transistor. The calculation results revealed that, by adjusting the electric potentials at the ends of the nanochannels, the ionic current could be (1) cut off, (2) regulated in the main channel, (3) diverged into the main and subchannels, (4) turned from the main channel to the subchannel, and (5) merged into the subchannel. A series connection of this nanofluidic system can therefore be used in biotechnological applications for electrophoretic separation and for sorting of ions and biomolecules.

DOI: 10.1103/PhysRevE.78.026301 PACS number(s): 47.61.Fg

I. INTRODUCTION

When the dimensions of a nanofluidic channel with surface charge are comparable to the Debye length, ionic current can be controlled by using the field effect because the channel is substantially filled with a unipolar solution of counterions due to ion screening at the channel entrance [1–3]. Analogous to control in metal-oxide-semiconductor field-effect transistors (MOSFETs), field-effect control of ionic current has been demonstrated in nanofluidic devices [4,5]. However, it is not a required condition for controlling ionic current that the electrical double layers are overlapped and the channel is substantially filled with a unipolar solution of counterions [6]. If the channel has a junction at which the surface charge is spatially changed from positive to negative along the channel, an electric field applied along the channel induces accumulation or depletion of ions at the junction, resulting in ionic current control. This behavior is similar to that observed in various *p-n* junction devices, such as semiconductor diodes and bipolar membranes [7,8]. We proposed and modeled a current-rectifying nanofluidic diode in which the two halves of a nanofluidic channel have opposite surface charge [9], and the current rectification was demonstrated experimentally in a nanofluidic diode with known channel dimensions and surface charge [10] in which first the nanochannel was fabricated using a sacrificial polysilicon process [4,11] and then the surface charge was modified by the diffusion-limited patterning (DLP) method [12]. The measured ionic currents agreed well with the theoretical predictions except at ultralow ion concentration (<100 μM). Ion current rectification also occurs in asymmetric nanopores when the characteristic length scale is of the order of the Debye length or smaller. Siwy and co-workers have studied ion current rectification in a conically shaped system both theoretically and experimentally [13,14].

Prior research on ion transport through nanochannels has mainly dealt with straight nanochannels and the intersections between a nanochannel and a microchannel [15–18], and only a few have dealt with ion transport through an intersection of nanochannel [19–22]. To our knowledge, ion transport through an intersection of nanochannels with surface charge distribution has not yet been investigated even though such intersections are expected to have unique transport characteristics advantageous for the control of ionic current. For example, because surface charge affects the ion concentration in a nanofluidic channel, if the surface charge is distributed around the intersection, then the ion concentration could also be distributed around the intersection. Thus, nonlinear control of ionic current through an intersection should be achievable by adjusting the electric potential at the end of nanofluidic channels. The first step toward more complicated nanofluidic circuits [23] is to clarify the transport characteristics through such intersections.

In this study, we proposed and modeled a nanofluidic bipolar transistor consisting of a T-intersection of two silica nanochannels with surface charge distribution. This model system is equivalent to a *p-n-p* transistor used in a common-emitter circuit. Semiconductor bipolar transistors are typically used in electrical applications for current amplification and switching, whereas the nanofluidic bipolar transistor proposed here might be used in biotechnological applications for switching, regulation, and turn of the flow of ions and biomolecules. Also in this study, we extended the model system to a series connection of three nanofluidic bipolar transistors and a nanofluidic diode to determine its application to multifunctional nanofluidic circuits.

II. METHODOLOGY

In the analysis of ion transport in a nanofluidic bipolar transistor consisting of a T-intersection of two nanofluidic channels, the governing equations are the Poisson-Nernst-Planck equations and the Stokes equations as follows:

$$\nabla^2 \phi = -\frac{\rho_e}{\epsilon_0 \epsilon}, \tag{1}$$

$$\nabla \cdot \mathbf{J}_a = 0, \tag{2}$$

$$\nabla \cdot \mathbf{u} = 0, \tag{3}$$

$$-\nabla p + \mu \nabla^2 \mathbf{u} - \rho_e \nabla \phi = 0, \tag{4}$$

 ©2008 The American Physical Society

where ϕ is electrostatic potential, n_a is concentration of ion species a, p is pressure and $\mathbf{u}$ is the velocity vector, ϵ_0 is the permittivity of vacuum, ϵ is dielectric constant of the medium, and μ is fluid viscosity. Here, ρ_e is the net charge density and is given by $\rho_e=\Sigma_a z_a e n_a$, where z_a and e are the valence of ion species a and electronic charge, respectively, and $\mathbf{J}_a$ is the flux of ion species a and is given by $\mathbf{J}_a=-D_a[\nabla n_a+(z_a e n_a/kT)\nabla\phi]+n_a\mathbf{u}$, where D_a, k and T are diffusivity of ion species a, Boltzmann's constant, and temperature, respectively. The boundary conditions at the walls of channels and reservoirs and at the ends of reservoirs are given as follows:

$$\nabla_\perp \phi = -\frac{\sigma}{\epsilon_0 \epsilon}, \quad J_{a\perp} = 0,$$

$$\mathbf{u} = 0 \quad \text{(at channel and reservoir walls)}, \tag{5}$$

$$\phi = \phi_{\text{bulk}}, \quad n_a = n_{\text{bulk}}, \quad \nabla_\perp \mathbf{u} = 0,$$

$$p = 0 \quad \text{(at reservoir ends)}, \tag{6}$$

where $\perp$ and bulk denote the component normal to the boundary and bulk value, respectively, and σ is the surface charge density. Equations (1)–(4) are solved under the boundary conditions (5) and (6) using a finite difference algorithm, yielding ϕ, n_a, p, and $\mathbf{u}$ in the system. If ϕ, n_a, p, and $\mathbf{u}$ are known, the current of the ion species a can then be obtained by integrating the current density over the cross section

$$\mathbf{I}_a = \int_S z_a e \mathbf{J}_a dS, \tag{7}$$

where S is the cross sectional area of the channel.

Figure 1(a) shows the 2D calculation system of a nanofluidic bipolar transistor consisting of two nanochannels (i.e., main channel, L_x long and L_y wide, and a subchannel, l_y long and l_x wide) and three square reservoirs (i.e., emitter, base, and collector reservoirs), one at each end of the main channel and at the end of the subchannel. Because the real device is 3D, 2D approximation implies that the third dimension has large value and either main or subchannel has two nanoscale dimensions. In this study, 2D approximation is assumed to simply understand the characteristics of this nanofluidic device. In the design of a practical device, constraints in the third direction and/or complex structure could be needed. However, the characteristics of ionic flow will not be changed by further constraints and/or more complex structure because ionic flow inside nanofluidic channels is mainly governed by its electrophoretic mobility and not governed by the advection due to fluid flow, e.g., electroosmotic flow and pressure-driven flow. The length of the base region in the main channel is L_{bx}, and the surface charge density σ in the base region, that is, in the middle part of the main channel and in the entire subchannel, is $+\sigma$ ($\sigma>0$) and that in the main channel outside the base region is $-\sigma$. At the wall faces of the reservoirs, $\sigma=0$. Figure 1(b) shows an equivalent p-n-p transistor used in the common-emitter circuit. In a semiconductor bipolar transistor, holes and electrons are the major charge carriers in p- and n-type semiconductors, respectively, whereas in a nanofluidic bipolar transistor, cations and anions are the major charge carriers in nanofluidic channels with negatively and positively charged walls, respectively. When the dimensions of nanofluidic channels are increased relative to the Debye length, the difference in concentration between major and minor charge carriers decreases, although the ionic current in a straight nanofluidic channel can still be controlled at the junctions between positively and negatively charged walls [9]. In the calculations, we assumed $L_x=5$ μm, $L_y=30$ nm, $l_y=5$ μm, $l_x=15$ nm, $L_{bx}=500$ nm, $\sigma=2$ mC/m^2, and each reservoir was 1×1 μm^2. Each reservoir was assumed filled with 5 mM KCl aqueous solution ($n_{\text{bulk}}=5$ mM) and the distribution and transport of cations (K^+) and anions (Cl^-) in a nanofluidic bipolar transistor were calculated as a function of the base potential ϕ_b at fixed emitter and collector potentials $\phi_e=5$ V and $\phi_c=0$ V. The physical properties of the ions [24] and fluid were assumed $D_{K^+}=1.96\times 10^{-9}$ m^2/s, $D_{Cl^-}=2.03\times 10^{-9}$ m^2/s, $\epsilon=80$, and $\mu=10^{-3}$ Pa s.

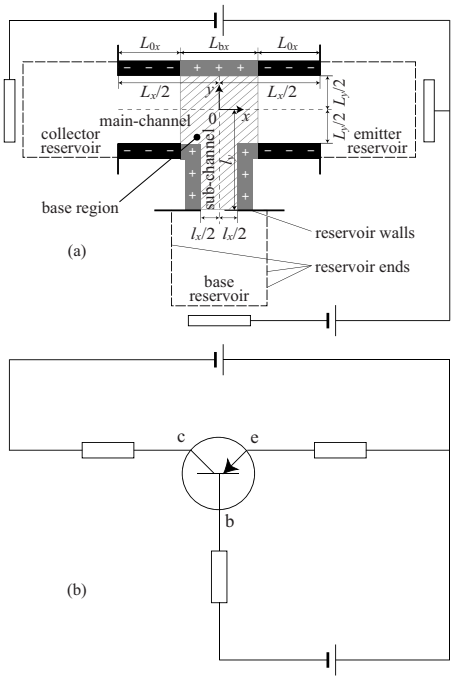

FIG. 1. (a) 2D calculation system and schematic of a nanofluidic bipolar transistor consisting of two nanochannels (main channel with length $L_x=5$ μm and width $L_y=30$ nm) and a subchannel (length $l_y=5$ μm and width $l_x=15$ nm) with three 1×1 μm^2 reservoirs at the ends of the nanochannels and (b) an equivalent p-n-p transistor used in the common-emitter circuit. Surface charge density is 2 mC/m^2 in the base region (cross-hatching area), and is -2 mC/m^2 in the main channel outside the base region. Length of base region in the main channel is $L_{bx}=500$ nm.

III. RESULTS AND DISCUSSION

A. Single nanofluidic bipolar transistor

Figures 2(a)–2(d) show the calculated ϕ, n, and p profiles along the main and subchannels at four different $\phi_b=7$, 4, 0, and -40 V. The ϕ and p profiles are along $y=0$ and $x=0$ and

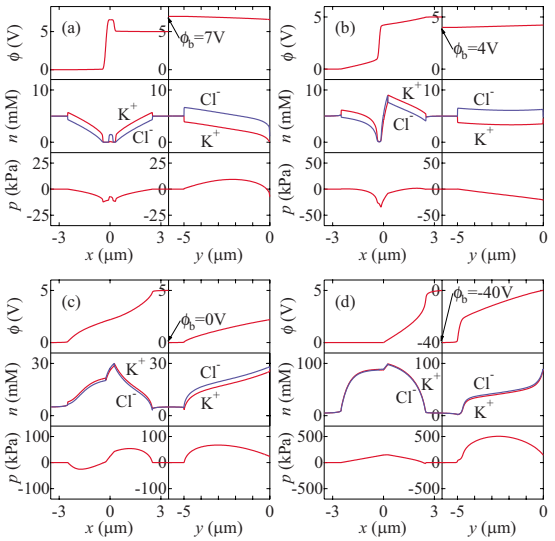

FIG. 2. (Color online) Calculated electric potential ϕ, ion concentration n, and pressure p profiles along the main and subchannels at four different base potentials: (a) ϕ_b=7 V, (b) ϕ_b=4 V, (c) ϕ_b=0 V, and (d) ϕ_b=−40 V. Electric potentials at emitter and collector are ϕ_e=5 V and ϕ_c=0 V, respectively, and bulk ion concentration is n_{bulk}=5 mM. The ϕ and p profiles are along y=0 and x=0 and n profiles are the averaged concentration (concentration averaged in the channel cross section) profiles along the x and y directions.

the n profile is the averaged concentration (i.e., concentration averaged in the channel cross section) profile along the x and y directions. At ϕ_b=7 V [Fig. 2(a)], two depletion regions appear at two ends of the base region in the main channel because at this ϕ_b, the system can be regarded as a combination of two reverse-biased nanofluidic diodes [9]. Therefore, the ionic currents both in the main and subchannels are near zero. At ϕ_b=4 V [Fig. 2(b)], depletion and accumulation regions respectively appear at the left and right ends of the base region in the main channel because at this ϕ_b, the system can be regarded as a combination of reverse- and forward-biased nanofluidic diodes. However, ions are not completely depleted from the left end because ions diffuse from the accumulation region (right end) to the depletion region (left end) across the base region in the main channel. In the subchannel, the electric potential gradient is almost zero, resulting in near-zero ionic current. Therefore, ionic current flows only in the main channel. At ϕ_b=0 V [Fig. 2(c)], ions accumulate at such a high concentration at the right end of the base region in the main channel that the Debye length in the solution λ becomes much smaller than the channel width (λ=2.15 nm in 20 mM KCl aqueous solution) and the potential barrier disappears at the left end and ions flow without any potential barrier both in the main and subchannels. Consequently, the emitter current I_e splits into a collector current I_c and base current I_b. At ϕ_b=−40 V [Fig. 2(d)], the electric potential gradient is near zero only in the left side of the main channel, suggesting that I_c is near zero and $I_e \approx I_b$.

Figure 3 shows the calculated I_c, I_b, and I_e as a function of ϕ_b. All three curves intersect the x axis (I=0) once, that is, I_c, I_b, and I_e become zero at $\phi_{I_{c0}}$=−40 V, $\phi_{I_{b0}}$=4 V, and

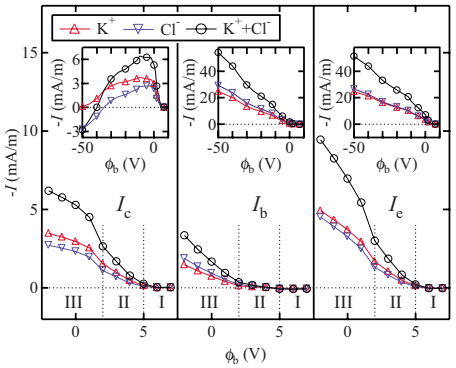

FIG. 3. (Color online) Calculated collector current I_c, base current I_b, and emitter current I_e as a function of base potential ϕ_b. Electric potentials at emitter and collector are ϕ_e=5 V and ϕ_c=0 V, respectively, and bulk ion concentration is n_{bulk}=5 mM. Insets show curves at −50 V≤ϕ_b≤7 V on an expanded scale. Regions I, II, III, respectively, correspond to the "cutoff," "forward active," and "saturation" regions in a semiconductor bipolar transistor.

$\phi_{I_{e0}}$=6 V, respectively, and $\phi_{I_{c0}} < \phi_{I_{b0}} < \phi_{I_{e0}}$. When $\phi_b > \phi_{I_{e0}}$, all three currents are near zero (region I). When $\phi_b \approx \phi_{I_{b0}}$, (around 2 V < ϕ_b < around 5 V), $I_b \approx 0$ and $I_e \approx I_c$, and both $|I_c|$ and $|I_e|$ increase with decreasing ϕ_b (region II). The gradients of I_c, I_b, and I_e with respect to ϕ_b change drastically at $\phi_b \approx 2$ V, when n at the intersection becomes so large that the potential barrier disappears and ions begin to flow without any potential barrier both in the main and subchannels. When $\phi_b < 2$ V, all three currents ($|I_e|$, $|I_b|$, and $|I_c|$) increase with decreasing ϕ_b (region III). However, with further decrease in ϕ_b, $|I_e|$, and $|I_b|$ increase, whereas $|I_c|$ decreases and then intersects the x axis ($|I_c|$=0) at $\phi_b = \phi_{I_{c0}}$ (see inset of Fig. 3). Regions I, II, III correspond, respectively, to "cutoff," "forward active," and "saturation" regions in a semiconductor bipolar transistor.

Figure 4 shows the calculated transport factor $\alpha(=I_c/I_e)$ and current gain $\beta(=I_c/I_b)$ as a function of base potential ϕ_b (squares and circles, respectively). α and β go to infinity at $\phi_b = \phi_{I_{e0}}$ and $\phi_{I_{b0}}$, respectively. At $\phi_b > \phi_{I_{e0}}$, $\alpha < 0$ and $\beta < 0$, suggesting that both of the nanochannels between emitter base and collector base can be regarded as a reverse-

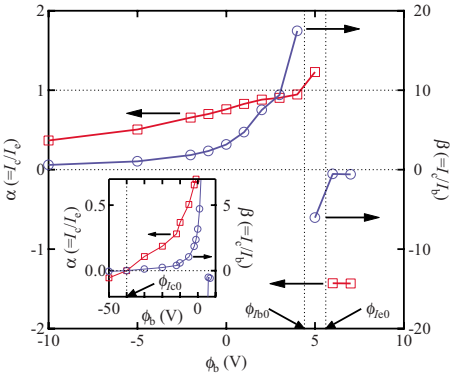

FIG. 4. (Color online) Calculated transport factor $\alpha(=I_c/I_e)$ (□) and current gain $\beta(=I_c/I_b)$ (○) as a function of base potential ϕ_b. Insets show curves at −50 V≤ϕ_b≤7 V on expanded scale.

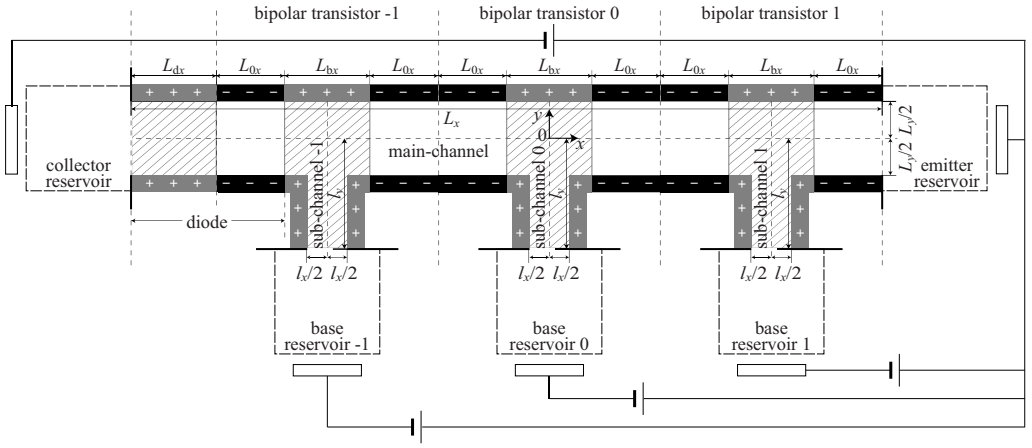

FIG. 5. Calculation system of series connection of three nanofluidic bipolar transistors and a nanofluidic diode consisting of a main channel with length L_x=17.5 μm and width L_y=30 nm and three subchannels of length l_y=5 μm and width l_x=15 nm, and with three 1 $\times$1 μm^2 reservoirs at the ends of nanochannels. Surface charge density σ is 2 mC/m^2 in the base region of the nanofluidic bipolar transistors and in the left part of a nanofluidic diode (crosshatched area), and is −2 mC/m^2 in the remainder of the main channel. Length of base region in the main channel is L_{bx}=500 nm and that of left part of a nanofluidic diode is L_{dx}=2.5 μm.

biased nanofluidic diode. Consequently, all currents could be cut off by increasing ϕ_b to above $\phi_{I_{e0}}$. At $\phi_{I_{b0}}<\phi_b<\phi_{I_{e0}}$, $\alpha>0$, and $\beta<0$, suggesting that I_e goes across the base region toward the collector reservoir but the nanochannels between collector base can still be regarded as a reverse-biased nanofluidic diode. At $\phi_{I_{c0}}<\phi_b<\phi_{I_{b0}}$, $\alpha>0$, and $\beta>0$, suggesting that I_e splits into I_c and I_b. At $\phi_b>2$ V, α is near unit, the nanofluidic bipolar transistor can be used to regulate the ionic current along the main channel. Whereas at $\phi_b<2$ V, α and β decrease rapidly with decrease in ϕ_b. At $\phi_b=\phi_{I_{c0}}$, $\alpha=\beta=0$, that is, I_e completely turns to I_b. At $\phi_b<\phi_{I_{c0}}$, $\alpha<0$, and $\beta<0$ again. But this time, both of the nanochannles between emitter base and collector base can be regarded as a forward-biased nanofluidic diode, and both I_e and I_c flow toward the base reservoir. In summary, there are five operation modes of ionic current in a single nanofluidic bipolar transistor: (1) cutoff, (2) regulation, (3) diversion, (4) turn, and (5) merge.

B. Series connection of nanofluidic bipolar transistors and a nanofluidic diode

Figure 5 shows the calculation system of three nanofluidic bipolar transistors and a nanofluidic diode connected in series. The surface charge of the left end of the main channel can be changed from negative to positive within a range of L_{dx} and thus this part of the main channel is regarded as the left part of a nanofluidic diode. The right part of a nanofluidic diode is overlapped by the collector side of the main channel in the left nanofluidic bipolar transistor. The main channel is L_x=17.5 μm long and L_y=30 nm wide, each of the three subchannels is l_y=5 μm long and l_x=15 nm wide, and each of the five reservoirs at the ends of the nanochannels is 1$\times$1 μm^2. In this series connection, σ=2 mC/m^2 in the base region of the nanofluidic bipolar transistors and in the left part of the nanofluidic diode, and σ=−2 mC/m^2 in the remainder of the main channel. The length of the base region in the main channel is L_{bx}=500 nm and that of the left part of the nanofluidic diode is L_{dx}=2.5 μm. In this study, the ionic current in this series-connection system was calculated for three of the five operation modes (cutoff, regulation, and turn) in a single nanofluidic bipolar transistor.

In the cutoff mode, the ionic current in the main channel is cut off by increasing one of the base potentials ϕ_{bi} (i=−1,0,1), above ϕ_e when the potential bias is applied between the emitter and collector reservoirs ($\phi_c<\phi_e$). In practical applications, if several channels share common emitter and collector reservoirs and the ionic current is controlled to flow in some channels and not to flow in the others, this operation mode can be used. Figure 6 shows the calculated ϕ, n, and p profiles along the main channel and three subchannels at ϕ_e=5 V, ϕ_c=0 V, ϕ_{b-1}=0 V, ϕ_{b0}=7 V, and ϕ_{b1}=5 V, and n_{bulk}=5 mM. The profiles in the main channel are similar to those of a single nanofluidic transistor [Fig. 2(a)] and the gradients of ϕ in the subchannels are near zero. The calculated ionic currents are near zero in all the chan-

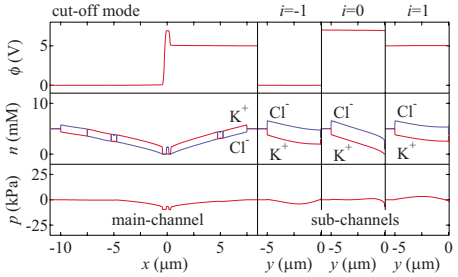

FIG. 6. (Color online) Calculated electric potential ϕ, ion concentration n, and pressure p profiles along the single main and three subchannels for cutoff mode in the series-connection system of three nanofluidic bipolar transistors and a nanofluidic diode. Electric potential at the reservoirs are ϕ_e=5 V, ϕ_c=0 V, ϕ_{b-1}=0 V, ϕ_{b0}=7 V, and ϕ_{b1}=5 V, and bulk ion concentration is n_{bulk}=5 mM. The ϕ and p profiles are along y=0 and $x_i=i\times(L_{bx}+2L_{0x})$ (i=−1,0,1) and n profiles are the averaged concentration (concentration averaged in the channel cross section) profiles along the x and y directions.

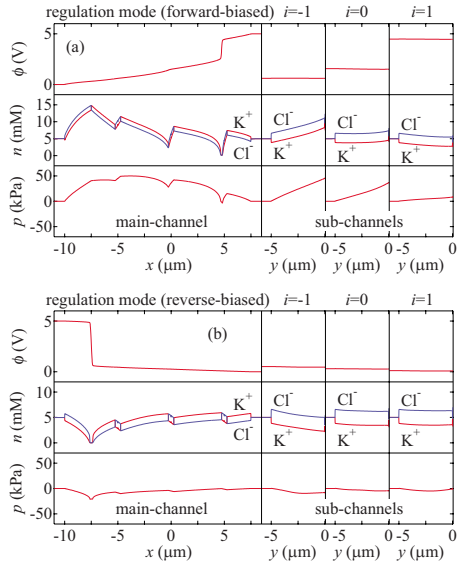

FIG. 7. (Color online) Calculated electric potential ϕ, ion concentration n, and pressure p profiles along the single main and three subchannels for cutoff mode in the series-connection system of three nanofluidic bipolar transistors and a (a) forward- and (b) reverse-biased nanofluidic diode. Electric potential at the reservoirs in the forward-direction are $\phi_e=5$ V, $\phi_c=0$ V, $\phi_{b-1}=0.617$ V, $\phi_{b0}=1.564$ V, and $\phi_{b1}=4.482$ V, and those in the reverse direction are $\phi_e=0$ V, $\phi_c=5$ V, $\phi_{b-1}=0.510$ V, $\phi_{b0}=0.303$ V, and $\phi_{b1}=0.107$ V, bulk ion concentration is $n_{\text{bulk}}=5$ mM. The ϕ and p profiles are along $y=0$ and $x_i=i\times(L_{bx}+2L_{0x})$ $(i=-1,0,1)$ and n profiles are the averaged concentration (concentration averaged in the channel cross section) profiles along the x and y directions.

nels. These calculation results indicate that the middle intersection is in the "off" state and the other two are in the "on" state, resulting in the zero ionic current. This situation is analogous to the "AND gate" in a logic circuit.

In the regulation mode, each base potential, ϕ_{bi} $(i=-1,0,1)$, should be nearly the same as the potential at each intersection between the main and subchannels, $\phi_{\text{int}i}$ $(i=-1,0,1)$, because the ionic current in the subchannel is near zero if the gradient of ϕ in the subchannel is zero [see Fig. 2(b)]. Each ϕ_{bi} was determined as follows. First, the governing equations were solved only for the main channel under the following boundary conditions at the entrance of the subchannels: $\nabla_y\phi=0$, $\nabla_y n_{K^+}=\nabla_y n_{Cl^-}=0$, $\nabla_y p=0$, $\mathbf{u}=0$ at $x_i-0.5l_x\leqslant x\leqslant x_i+0.5l_x$, and $y=-0.5L_y$, where $x_i=i\times(L_{bx}+2L_{0x})$ $(i=-1,0,1)$. Then, each ϕ_{bi} was set to the calculated ϕ at the middle of the entrance of the subchannel, i.e., $\phi_{bi}=\phi_{\text{int}i}=\phi(x_i,-0.5L_y)$, and the governing equations were solved for the entire calculation system. Note that a zero gradient of ϕ is not a sufficient condition for zero ionic current, and the value of $\phi_{\text{int}i}$ in the main-channel calculation is not the same as that in the entire system calculation. However, in the above procedure, the ionic current in the subchannel can be assumed near zero. Figures 7(a) and 7(b) show the calculated ϕ, n, and p profiles along the main channel and three subchannels for the forward and reverse directions in the nanofluidic diode, respectively. The electric potentials in the forward direction are $\phi_e=5$ V, $\phi_c=0$ V, $\phi_{b-1}=0.617$ V, $\phi_{b0}=1.564$ V, and $\phi_{b1}=4.482$ V, and those in the reverse direction are $\phi_e=0$ V, $\phi_c=5$ V, $\phi_{b-1}=0.510$ V, $\phi_{b0}=0.303$ V, and $\phi_{b1}=0.107$ V. The bulk ion concentration is $n_{\text{bulk}}=5$ mM. In the forward direction, the calculated ionic currents are $I_e=I_c=-0.52$ mA/m. $(I_{eK^+}=I_{cK^+}=-0.29$ mA/m, $I_{eCl^-}=I_{cCl^-}=-0.23$ mA/m) and all base currents are near zero. In the transistor, the profiles in the main channel are similar to those of a single nanofluidic transistor [Fig. 2(b)]. The gradients of ϕ in the subchannels are near zero, resulting in $I_b=0$. In the diode, ions accumulate and ϕ changes smoothly at the junction $(x=-7.5$ μm). In a straight nanofluidic bipolar transistor shown in our previous report [9], I is saturated with increasing potential bias between the emitter and collector $|\phi_e-\phi_c|$. However, in a nanofluidic bipolar transistor connected in series to a nanofluidic diode, I is not saturated due to the series connection of a forward-biased diode. In the reverse direction, the calculated ionic currents are $I_e=I_c=0.08$ mA/m $(I_{eK^+}=I_{cK^+}=0.05$ mA/m, $I_{eCl^-}=I_{cCl^-}=0.03$ mA/m) and all base currents are near zero. The depletion region appears at the junction of the diode $(x=-7.5$ μm), resulting in the suppression of I. In the regulation mode, the nanofluidic diode plays a role in the rectification of I.

In the turn mode, I_e is controlled to flow toward one of the three base reservoirs. Here, we considered one example, where I_e flows toward the middle base reservoir $(i=0)$. In this example, $\phi_e=1$ V, $\phi_c=0$ V, and ϕ_{b-1} was set at 0 V. The base potentials ϕ_{b0} and ϕ_{b1} were set so that I_e did not flow toward the left and right base reservoirs $(i=-1$ and 1). Specifically, ϕ_{b1} was set to $\phi_{\text{int}1}$ so that ionic current flowed only in the main channel, and ϕ_{b0} was set so that the ionic current did not flow toward the collector reservoir. First, ϕ_{b1} was determined using a procedure similar to that used in the regulation mode by assuming ϕ_{b0}, that is, the governing equations were solved except for the right subchannel, where the boundary conditions at the entrance of the right subchannel were assumed to be the same as those in the regulation mode. If the calculated ionic current in the main channel between the left and middle intersections, I_{m-10}, was zero, ϕ_{b1} was set to $\phi_{\text{int}1}$, and the governing equations were solved for the entire calculation system. If $I_{m-10}\neq 0$, the same procedures were repeated by assuming another value of ϕ_{b0}. Figure 8 shows the calculated ϕ, n, and p profiles along the main channel and three subchannels at $\phi_e=1$ V, $\phi_c=0$ V, $\phi_{b-1}=0$ V, $\phi_{b0}=-1.1$ V, and $\phi_{b1}=0.568$ V and $n_{\text{bulk}}=5$ mM. The calculated ionic currents are $I_e=-0.76$ mA/m $(I_{eK^+}=I_{eCl^-}=-0.38$ mA/m), $I_{b0}=-0.76$ mA/m $(I_{b0K^+}=-0.35$ mA/m and $I_{b0Cl^-}=-0.41$ mA/m), $I_{m-10}=0.00$ mA/m $(I_{m-10K^+}=-0.03$ mA/m and $I_{m-10Cl^-}=0.03$ mA/m), and I_c, I_{b-1}, I_{b1} and their ionic currents of K^+ and Cl^- $(I_{cK^+}, I_{cCl^-}, I_{b-1K^+}, I_{b-1Cl^-}, I_{b1K^+}$, and $I_{b1Cl^-})$ are near zero. The profiles in the main channel and the middle subchannel are similar to those of a single nanofluidic transistor [Fig. 2(d)]. The electric potential ϕ is constant in all the channels except for those between the emitter and middle base reservoirs, suggesting that I_c, I_{b-1}, and I_{b1} are near zero and that I_e completely turns into I_{b0}. Furthermore, the ion concentration inside the channels is higher than the bulk ion concentration. In such conditions, ionic current cannot be controlled by the on-off states that are analogous to the states in a logic circuit, but it can be controlled by satisfying the

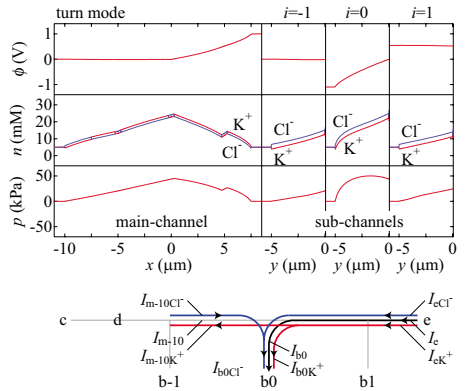

FIG. 8. (Color online) Calculated electric potential ϕ, ion concentration n, and pressure p profiles along the single main and three subchannels (top) and the current directions of K^+, Cl^-, and $K^+ + Cl^-$ (bottom) for turn mode in the series-connection system of three nanofluidic bipolar transistors and a nanofluidic diode. Electric potentials at the reservoirs are $\phi_e=1$ V, $\phi_e=0$ V, $\phi_{b-1}=0$ V, $\phi_{b0}=-1.1$ V, and $\phi_{b1}=0.568$ V, and the bulk ion concentration is $n_{\mathrm{bulk}}=5$ mM. The ϕ and p profiles are along $y=0$ and $x_i=i\times(L_{bx}+2L_{0x})$ $(i=-1,0,1)$ and n profiles are the averaged concentration (concentration averaged in the channel cross section) profiles along the x and y directions. Symbols "$b-1$," "$b0$," "$b1$," "c," and "e" denote left-base, middle-base, right-base, collector, and emitter reservoirs, respectively, and "d" denotes the diode.

conservation of ionic current at intersections (Kirchhoff's current law). Furthermore, the conservation of ionic current must be satisfied for each ion because the direction of each ionic current differs depending on diffusion, electroosmotic and pressure-driven flow, as shown in the lower panel of Fig. 8. The total ionic current ($K^+ + Cl^-$) is in the turn mode, whereas the ionic currents of K^+ and Cl^- are in the diversion and merge modes, respectively. In a series-connection nanofluidic system, the control of ionic current is complex if ions are concentrated inside the channels. In this study, the channel dimensions and the operation conditions have not yet been optimized, but three operation modes (cutoff, regulation, and turn) were demonstrated.

IV. CONCLUSIONS

In this study, ion distribution and transport in a single nanofluidic bipolar transistor and a series connection of three nanofluidic bipolar transistors and a nanofluidic diode were investigated. In a single nanofluidic bipolar transistor, the emitter, base, and collector ionic currents can be nonlinearly controlled by adjusting the base potential. There are five operation modes of ionic current in a single nanofluidic bipolar transistor: (1) cutoff, (2) regulation, (3) diversion, (4) turn, and (5) merge. In a series connection of three nanofluidic bipolar transistors and a nanofluidic diode, three operation modes were demonstrated: (1) cutoff, (2) regulation, and (3) turn. In the regulation mode, ionic current can be rectified by a nanofluidic diode. At low ion concentration [i.e., $\kappa_i L_y \approx 1$, where the Debye length of a KCl aqueous solution at the intersection λ_i $(=1/\kappa_i)$ is on the same order as the channel width L_y], ionic current can be controlled by the on-off states analogous to those in a logic circuit. In contrast, at high ion concentration (i.e., $\kappa_i L_y \gg 1$), ionic current can be controlled by satisfying the conservation of ionic current at each intersection (Kirchhoff's current law).

ACKNOWLEDGMENTS

This research was supported by the Japanese Ministry of Education, Culture, Sports, Science and Technology, Grant-in-Aid for Young Scientists (B) No. 18760139, 2007.

[1] A. J. Bard and L. R. Faulkner, *Electrochemical Methods* (Wiley, New York, 1980).
[2] M. Nishizawa, V. P. Menon, and C. R. Martin, Science **268**, 700 (1995).
[3] H. Daiguji, P. Yang, and A. Majumdar, Nano Lett. **4**, 137 (2004).
[4] R. Karnik, R. Fan, M. Yue, D. Li, P. Yang, and A. Majumdar, Nano Lett. **5**, 943 (2005).
[5] R. Karnik, K. Castelino, and A. Majumdar, Appl. Phys. Lett. **88**, 123114 (2006).
[6] D. Stein, M. Kruithof, and C. Dekker, Phys. Rev. Lett. **93**, 035901 (2004).
[7] B. Lovrecek, A. Despic, and J. O. M. Bockris, J. Phys. Chem. **63**, 750 (1959).
[8] H. D. Hurwitz and R. Dibiani, J. Membr. Sci. **228**, 17 (2004).
[9] H. Daiguji, Y. Oka, and K. Shirono, Nano Lett. **5**, 2274 (2005).
[10] R. Karnik, C. Duan, K. Castelino, H. Daiguji, and A. Majumdar, Nano Lett. **7**, 547 (2007).
[11] R. Karnik, K. Castelino, R. Fan, P. Yang, and A. Majumdar, Nano Lett. **5**, 1638 (2005).
[12] R. Karnik, K. Castelino, C. Duan, and A. Majumdar, Nano Lett. **6**, 1735 (2006).
[13] I. Vlassiouk and Z. S. Siwy, Nano Lett. **7**, 552 (2007).
[14] D. Constantin and Z. S. Siwy, Phys. Rev. E **76**, 041202 (2007).
[15] T. Kuo, D. M. Jr. Cannon, M. A. Shannon, P. W. Bohn, and J. V. Seedler, Sens. Actuators, A **102**, 223 (2003).
[16] T. Kuo, D. M. Jr. Cannon, Y. Chen, J. J. Tulock, M. A. Shannon, J. V. Sweedler, and P. W. Bohn, Anal. Chem. **75**, 1861 (2003).
[17] A. Chatterjee, D. M. Cannon Jr., E. Gatimu, J. V. Sweedler, N. R. Aluru, and P. W. Bohn, J. Nanopart. Res. **7**, 507 (2005).
[18] Y. Wang, A. L. Stevens, and J. Han, Anal. Chem. **77**, 4293 (2005).
[19] R. Karlsson, A. Karlsson, and O. Orwar, J. Am. Chem. Soc. **125**, 8442 (2003).
[20] J. H. Park, S. B. Sinnott, and N. R. Aluru, Nanotechnology **17**, 895 (2006).
[21] R. Riehn, R. H. Austin, and J. C. Sturm, Nano Lett. **6**, 1973 (2006).
[22] M. L. Kovarik and S. C. Jacobson, Anal. Chem. **79**, 1655 (2007).
[23] R. Mukhopadhyay, Anal. Chem. **78**, 7379 (2006).
[24] B. Hille, *Ion Channels of Excitable Membrane*, 3rd ed. (Sinauer Associates Inc., Sunderland, MA, 2001).